

Supporting information for

Single crystal growth of water-soluble metal complexes with
the help of the Nano-Crystallization method

Ricardo Alvarez, Philipp Nievergelt, Ekaterina Slyshkina, Peter Müller, Roger
Alberto, Bernhard Spingler*

Department of Chemistry, University of Zurich, 8057 Zurich, Switzerland

* Corresponding author: spingler@chem.uzh.ch

Figure S1 ¹H-NMR (D₂O) of cobalt(III) tris(2,2'-bipyridine) chloride (1).

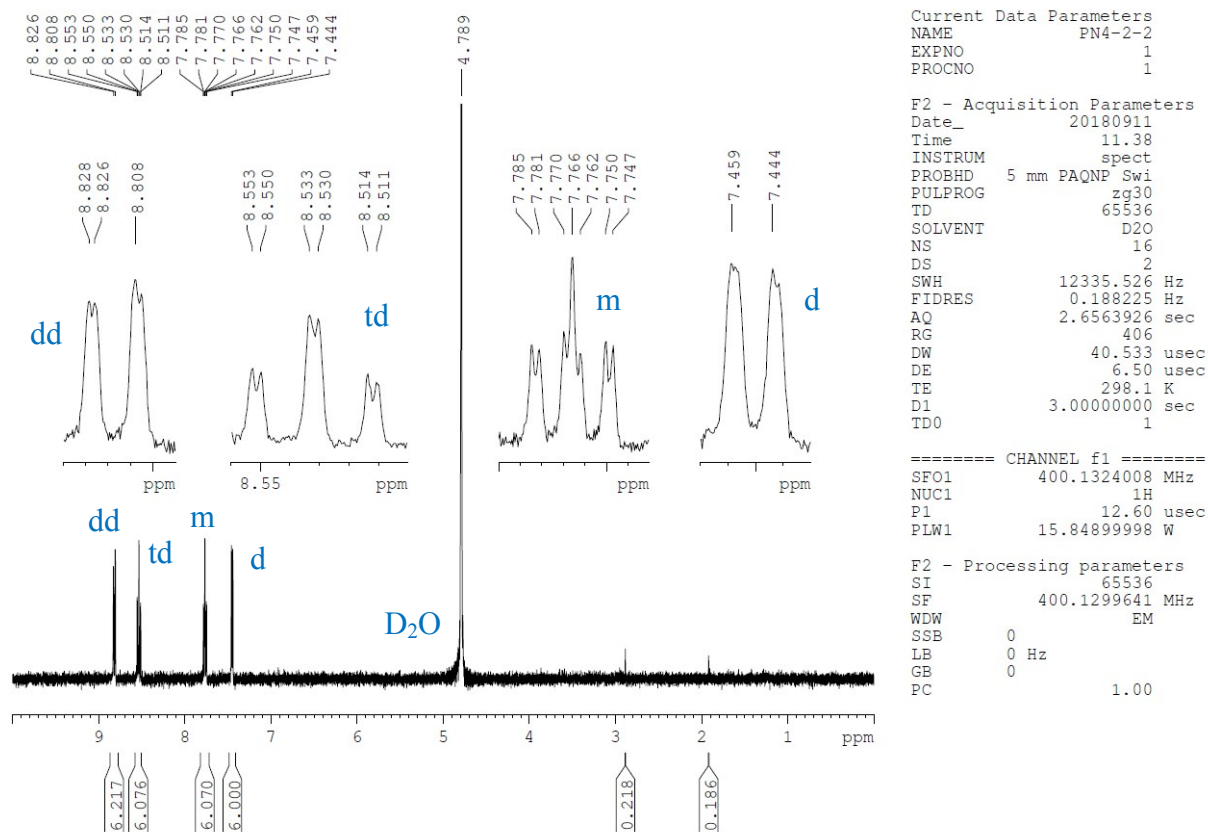


Figure S2 Simulated powder pattern of $[\text{Co(III)(bpy)}_3]\text{Cl}_3 \cdot 4(\text{H}_2\text{O})$ (**1**) with help of the Mercury software¹ based on the single crystal structure of **1**.

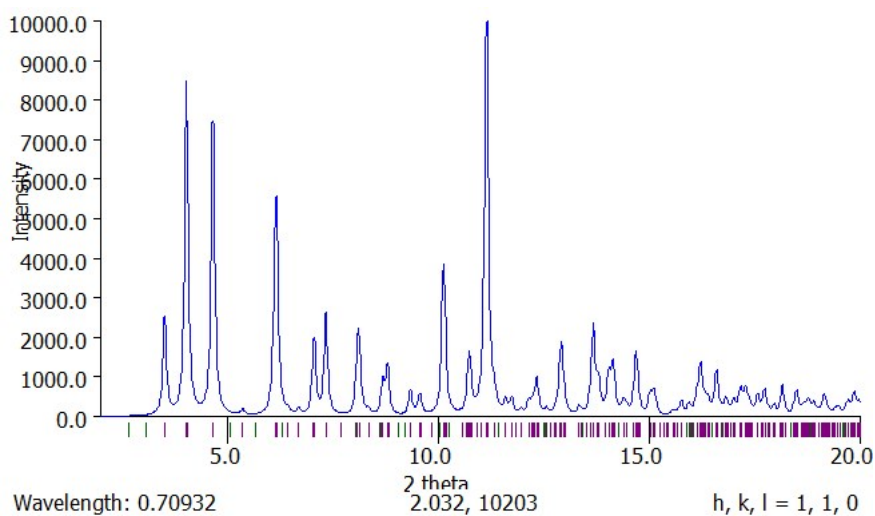
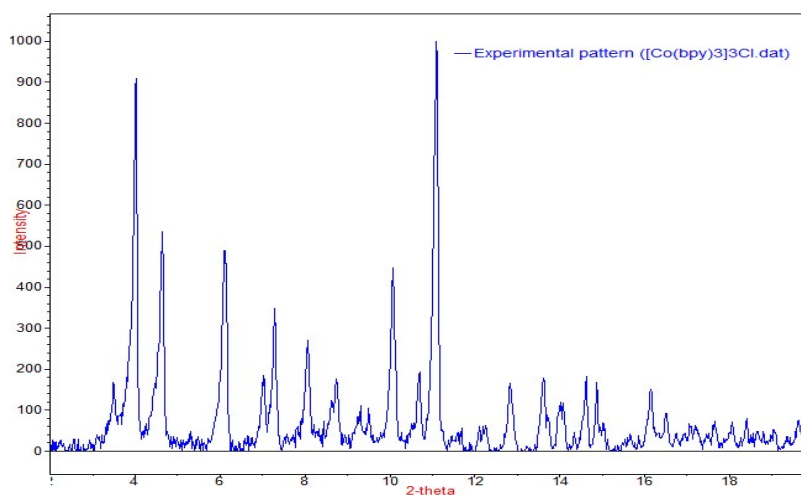


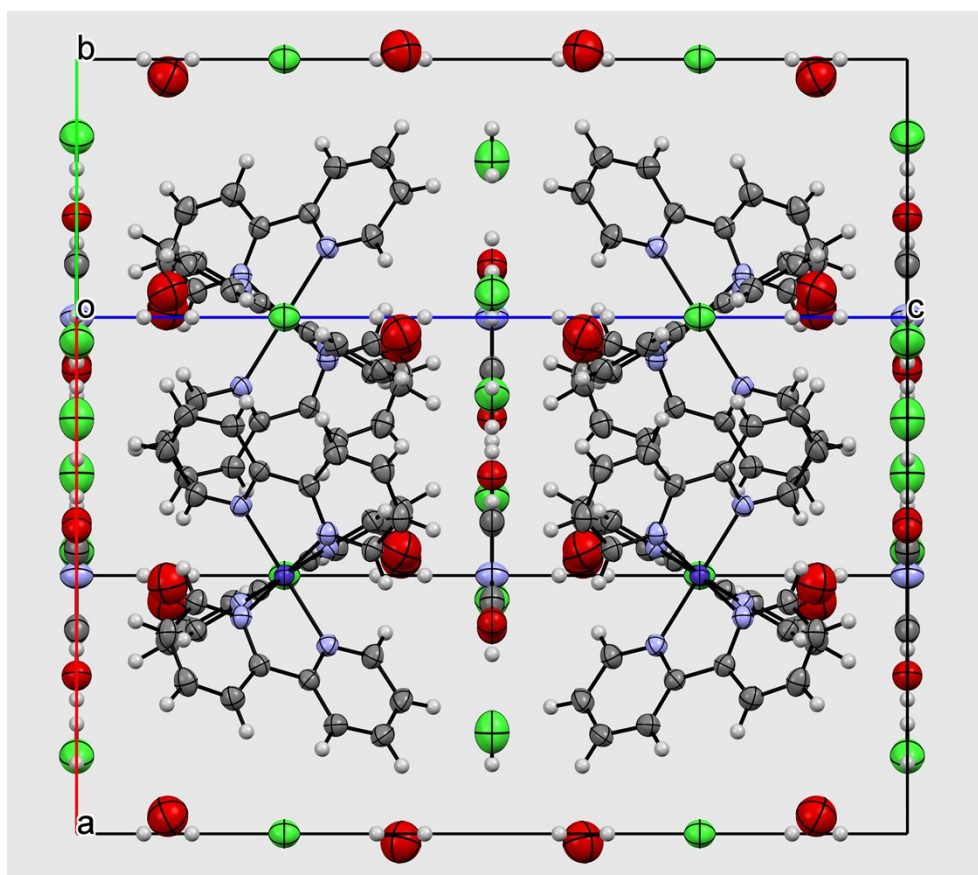
Figure S3 Measured PXRD pattern of **1**.



S1 Cobalt(II) tris(2,2'-bipyridine) dicyanamide chloride · tetrahydrate (1a)

Single crystals of **1a** were obtained with help of the high throughput screening method for nanocrystallization of salts by vapor diffusion at 20 °C of 500 nL of a 90% saturated solution of **1** in water mixed with the same volume of a 0.7 M solution of sodium dicyanamide against a reservoir of a 0.7 M solution of sodium dicyanamide. The crystallographic data are summarized in Table S1. In order to minimize the X-ray fluorescence caused by the cobalt complex being irradiated with copper radiation², a 7 keV threshold was applied for the hybrid pixel Pilatus detector.³ **1a** crystallized in the hexagonal space group *P6/mcc*. The tris-bipyridine cobalt(II) cation and the dicyanamide are both sitting on a three-fold symmetry axis (Figure 1). The two cyano groups of the dicyanamide and one water molecule occupy common positions and are therefore disordered in a ratio 67:33.

Figure S4 Packing diagram of **1a**.



S2 Cobalt(III) bis(2,2'-bipyridine) DL-malate · 10 hydrate (**1b**)

Single, red crystals of **1b** were obtained from the high throughput screening method for nanocrystallization of salts by vapor diffusion at 20°C of 500 nL of a 90% saturated solution of **1** in water mixed with the same volume of a 2.27 M solution of disodium DL-malate against a reservoir of a 2.27 M solution of disodium DL-malate. The crystallographic data are summarized in Table S1. During crystallization a ligand exchange took place in which one 2,2'-bipyridine ligand was replaced by a D- or L-malate anion. The resulting cobalt(III) bis(2,2'-bipyridine) DL-malate crystallized in the monoclinic space group $I2/a$. The asymmetric unit consists of half a molecule of cobalt(III) bis(2,2'-bipyridine) malate and 5 water molecules. The other half of the molecule is generated by the two-fold rotational axis of the space group, which passes through the Co-atom and the malate ligand, thereby indicating that part of the malate ligand is disordered. The D- and L-malate are coordinated as a bidentate trianion to the cobalt. The neighboring water molecules are disordered in a ratio of 50:50.

Additionally to **1b**, the crystallization also yielded the known yellow crystals of the starting material cobalt(III) tris(2,2'-bipyridine) chloride tetrahydrate (**1**)⁴ (Figure S6).

Figure S5 Packing diagram of **1b**.

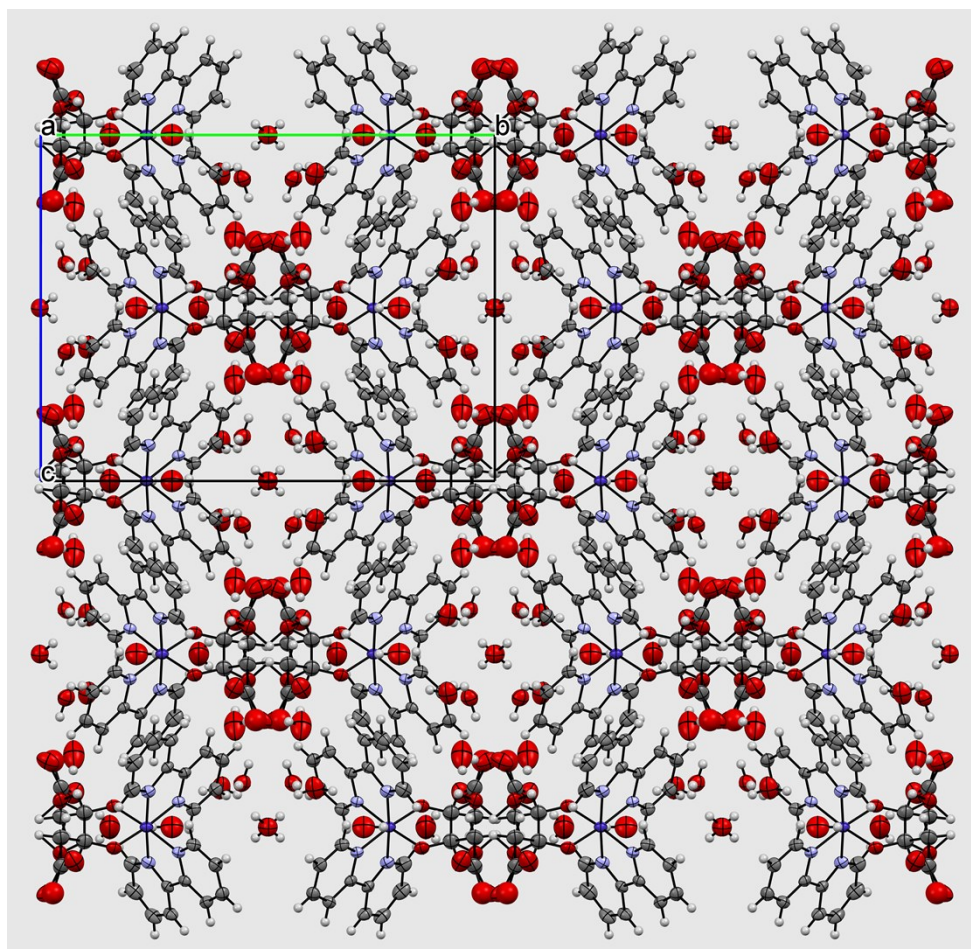
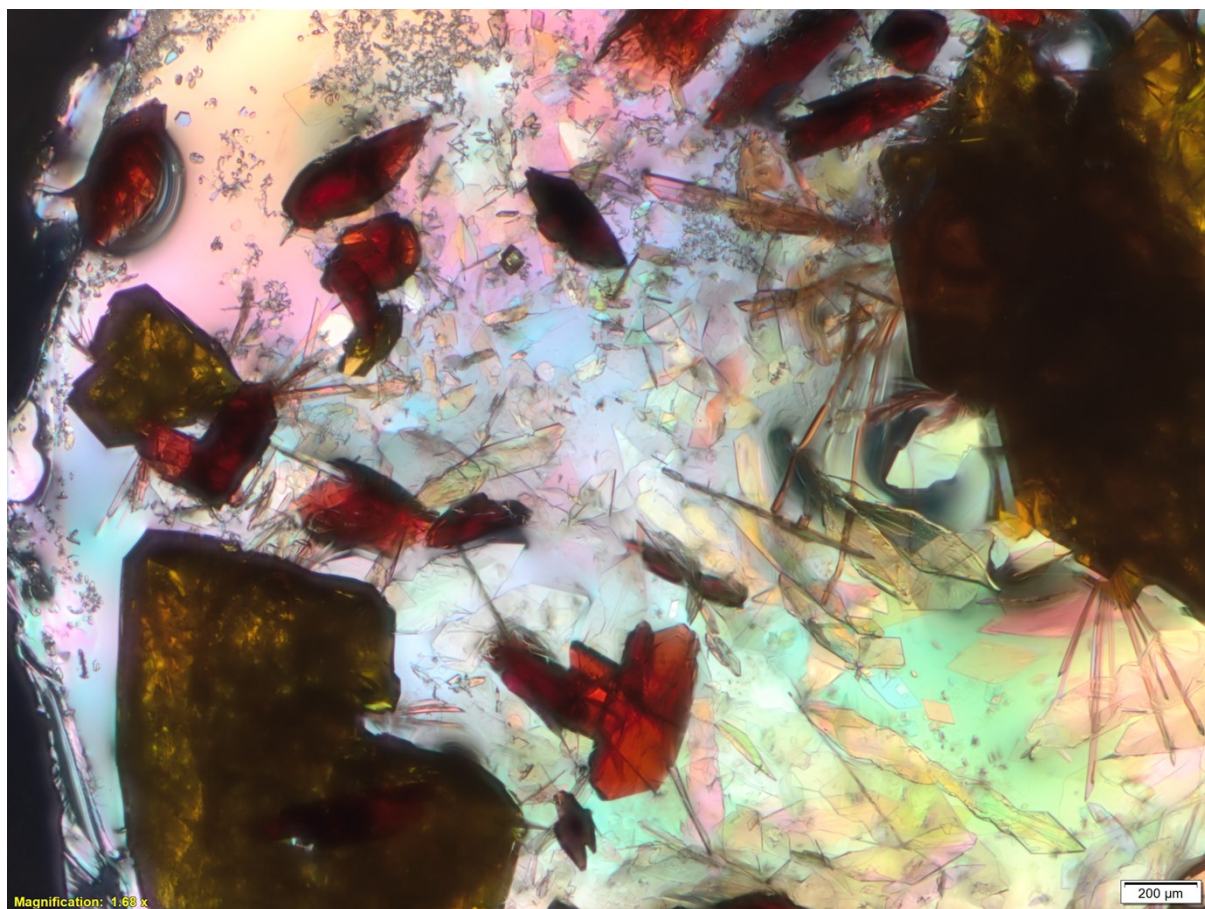


Figure S6 Crystallization of red **1c** and yellow **1** in a 36 μL sitting drop.



S3 Cobalt(III) bis(2,2'-bipyridine) L-malate · 9.25 hydrate · 0.25 sodium chloride (1c)

Single, red crystals were obtained from the high throughput screening method for nano-crystallization of salts by vapor diffusion at 20 °C of 500 nL of a 90% saturated solution of **1** in water mixed with the same volume of a 2.92 M solution of disodium L-malate against a reservoir of a 2.92 M solution of disodium L-malate. The crystallographic data are summarized in Table S1. During crystallisation a ligand exchange took place whereby one 2,2'-bipyridine ligand was replaced with one trianionic L-malate molecule. The resulting cobalt(III) bis(2,2'-bipyridine) L-malate crystallised in the triclinic, chiral space group P1. The asymmetric unit consists of one delta and one lambda molecule of cobalt(III) bis(2,2'-bipyridine) L-malate, half a chloride anion, half a sodium cation and 18.5 water molecules. A half-occupied water molecule and the half-occupied chloride anion occupy the same crystallographic site.

Additionally to **1c**, the crystallization also yielded the known yellow crystals of the starting material cobalt(III) tris(2,2'-bipyridine) chloride tetrahydrate (**1**)⁴ (Figure S8). Repeating the crystallization experiment with a 2.27 M L-malate solution (same malate concentration as used with DL-malate for the crystallization of **1b**) yielded again both complexes (Figure S9).

Figure S7 Packing diagram of **1c**.

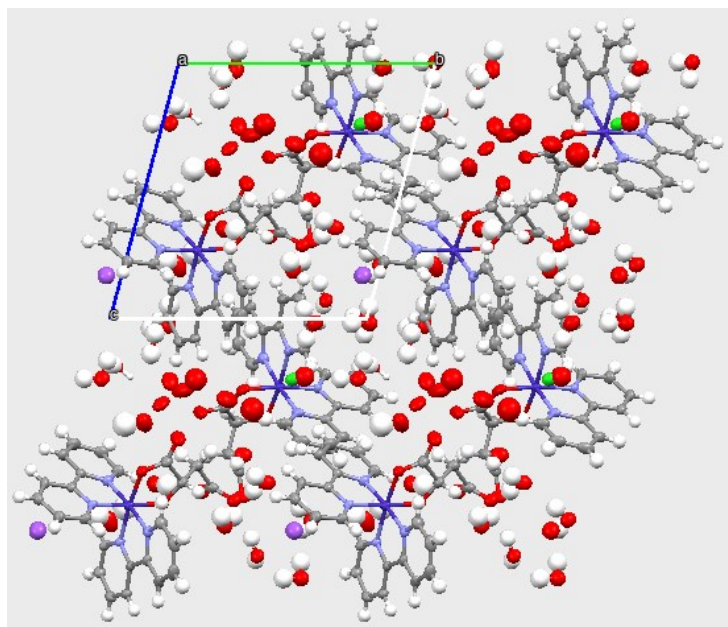


Figure S8 Crystallization of red **1c** and yellow **1** in a 36 μL sitting drop.

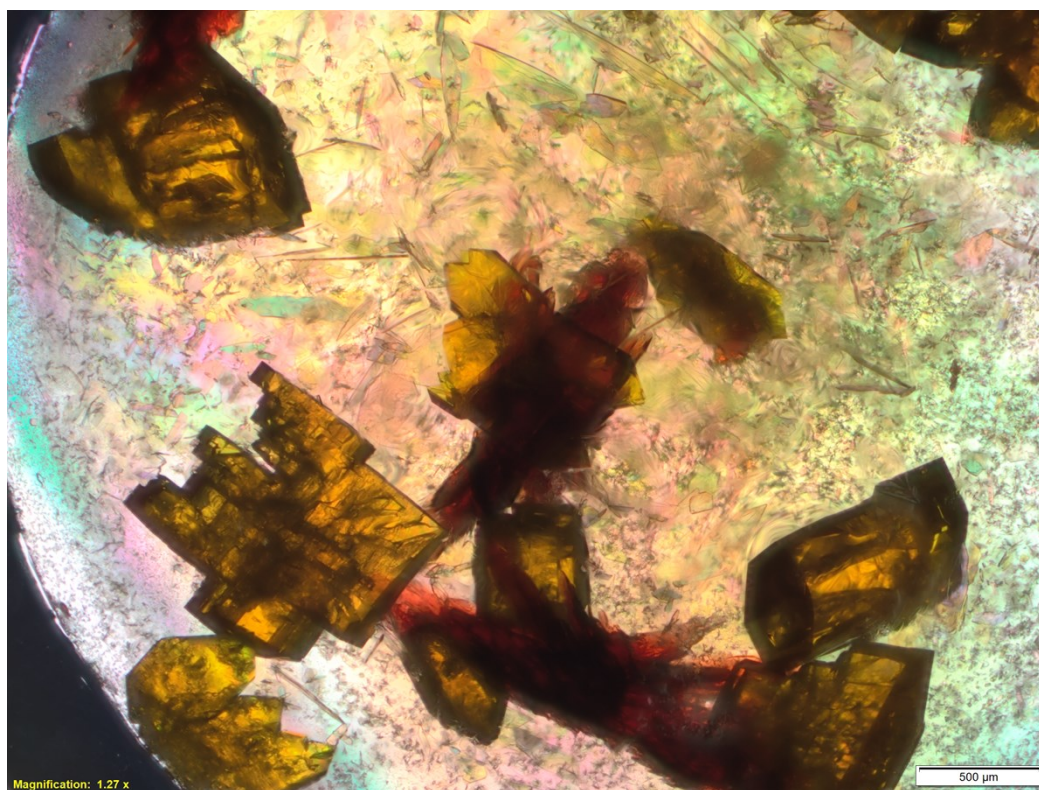
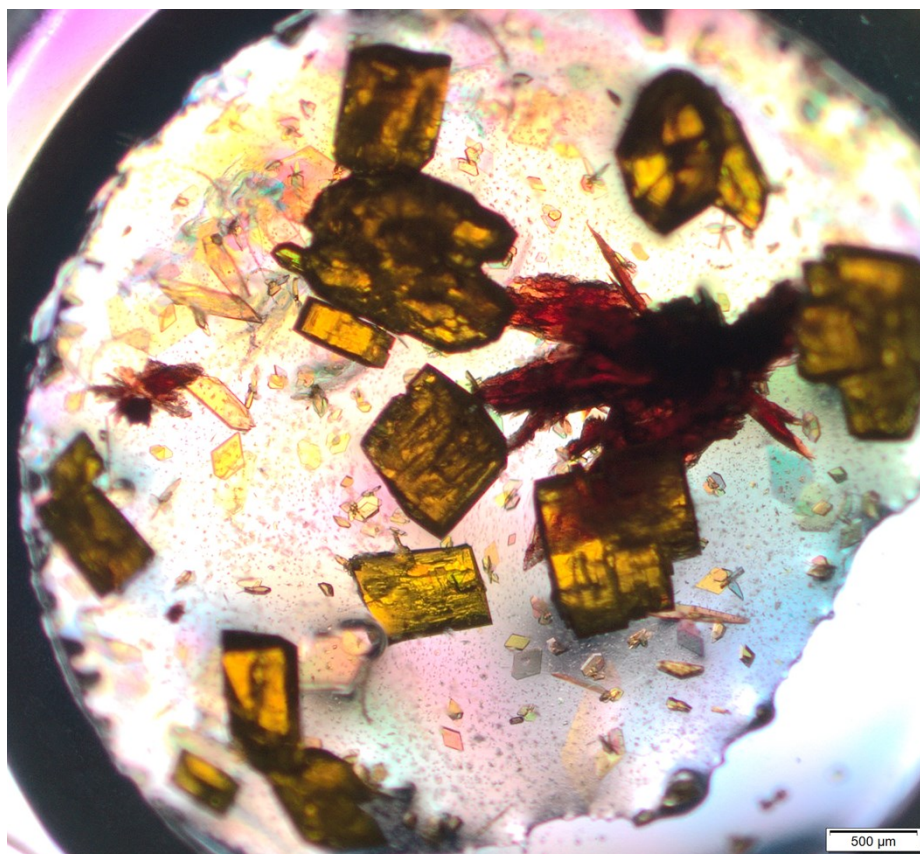


Figure S9 Crystallization of red **1c** and yellow **1** in a 36 μL sitting drop using a 2.27 M L-malate solution.



S4 Ruthenium(II) tris(4,4'-dimethyl-2,2'-bipyridine) hydrogenfumarate hemifumarate tetrahydrate (2a)

Single crystals of **2a** were obtained from the high throughput screening method for nano-crystallization of salts by vapor diffusion at 20°C of 500 nL of a 90% saturated solution of **2** in water mixed with the same volume of a 0.73 M solution of disodium fumarate against a reservoir of a 0.73 M solution of disodium fumarate. The crystallographic data are summarized in Table S2. **2a** crystallized in the monoclinic space group $P2_1/n$. The asymmetric unit consists of one ruthenium(II) tris(4,4'-dimethyl-2,2'-bipyridine) cation, one hydrogenfumarate anion, half a fumarate dianion, which sits across an inversion center, and four water molecules. The remaining ill-defined electron density had to be treated with the SQUEEZE procedure within *Platon*.⁵

Macroscopic synthesis of **2a** was done by vapor diffusion at 20°C of 200 μ L of a 90% saturated solution of **2** in water mixed with the same volume of a 0.73 M solution of disodium fumarate against 1.8 mL of a 0.73 M solution of disodium fumarate. The obtained material was analysed by PXRD (Figure S12), it mainly contained **2a** but also an unknown impurity.

Figure S10 Packing diagram of **2a**.

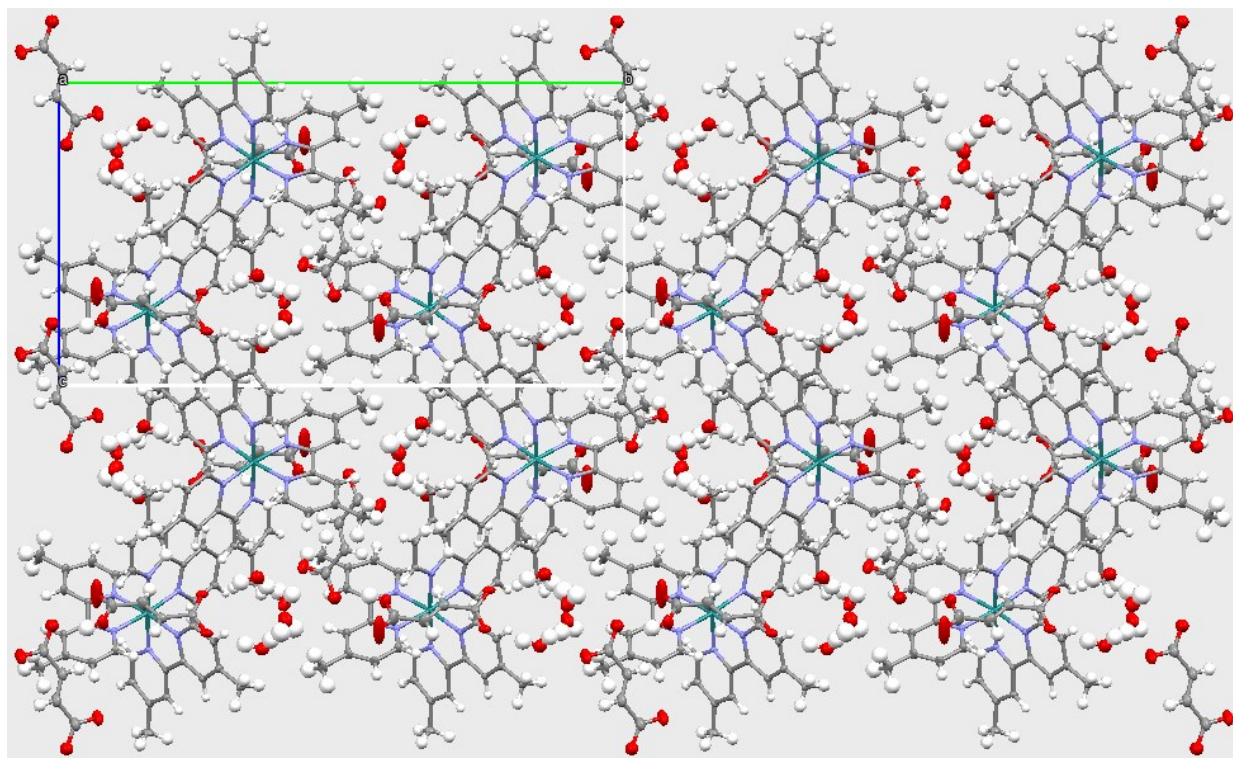


Figure S11 Simulated powder pattern of **2a** with help of the Mercury software¹ based on the single crystal structure of **2a**.

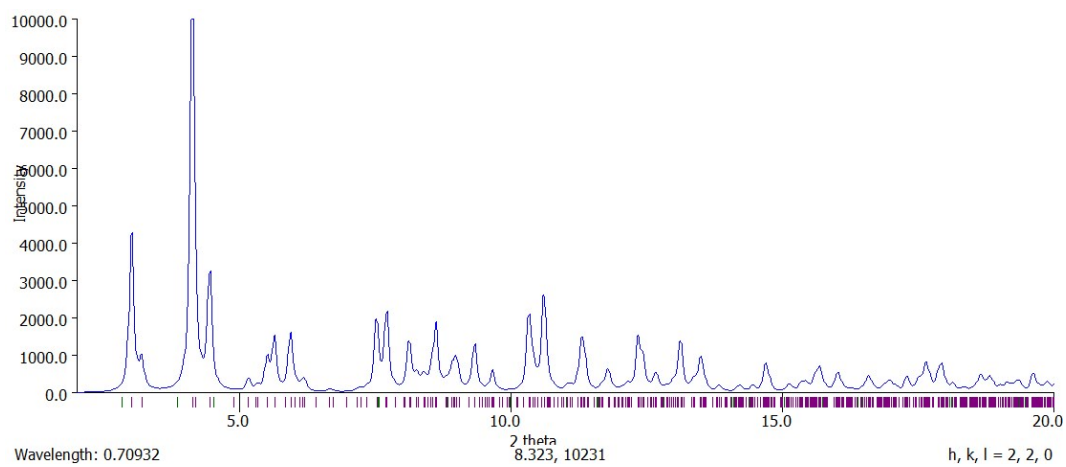
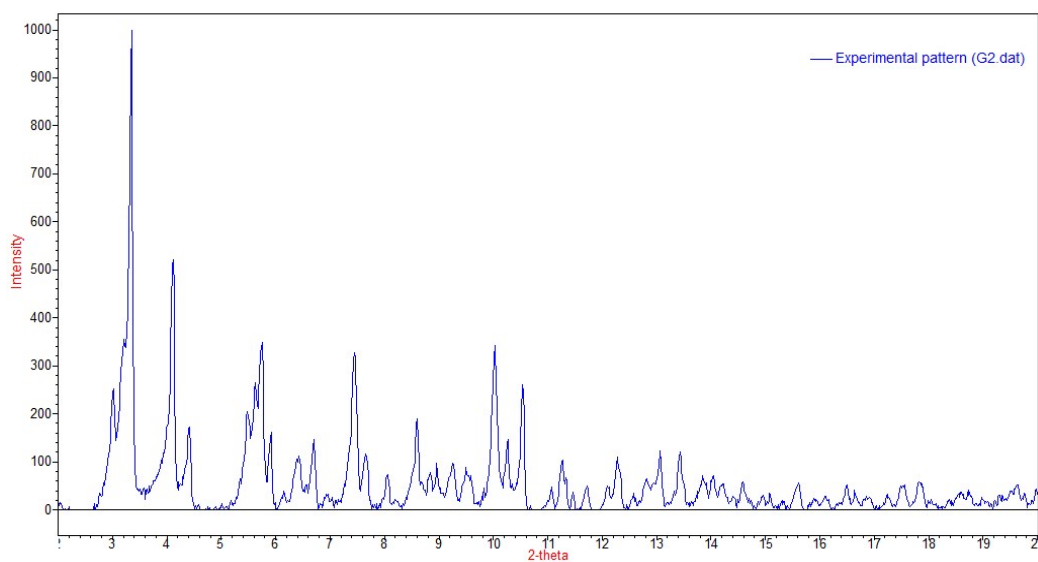


Figure S12 Measured PXRD pattern of **2a** synthesized on a macroscopic scale as described above.



S5 Ruthenium(II) tris(4,4'-dimethyl-2,2'-bipyridine) saccharinate tetrahydrate (**2b**)

Single crystals of **2b** were obtained from the high throughput screening method for nano-crystallization of salts by vapor diffusion at 20°C of 500 nL of a 90% saturated solution of **2** in water mixed with the same volume of a 1.57 M solution of sodium saccharinate against a reservoir of a 1.57 M solution of sodium saccharinate. The crystallographic data are summarized in Table S2. **2b** crystallized in the triclinic space group $P\bar{1}$. The asymmetric unit consists of one ruthenium(II) tris(4,4'-dimethyl-2,2'-bipyridine) cation, two saccharinate anions and four water molecules.

A macroscopic synthesis of **2b** was done as follows: The column for the ion exchange was packed with Dowex X1 (Fluka) in H₂O. Subsequently, the column was loaded with saccharinate ions (50 mL, saturated aq. solution of saccharin sodium salt). Then, ruthenium(II) tris(4,4'-dimethyl-2,2'-bipyridine) dichloride tetrahydrate (**2**, 101.1 mg, 0.127 mmol) was dissolved in H₂O (20 mL), passed through the column and dried under reduced pressure to yield ruthenium(II) tris(4,4'-dimethyl-2,2'-bipyridine) disaccharinate · 4.5 hydrate (**2b**, 116.4 mg, 0.106 mmol) as red crystals (yield: 84%).

IR (neat): 3050_w, 2919_w, 1619_m, 1579_m, 1478_w, 1447_w, 1329_w, 1257_m, 1138_m, 1116_m, 946_m, 832_m, 760_m.

EA: calcd. for C₅₀H₄₄N₈O₆RuS₂(H₂O)_{4.5}: C: 54.63, H: 4.86, N: 10.19; found: C: 54.57, H: 4.90, N: 10.35.

Figure S13 Packing diagram of **2b**.

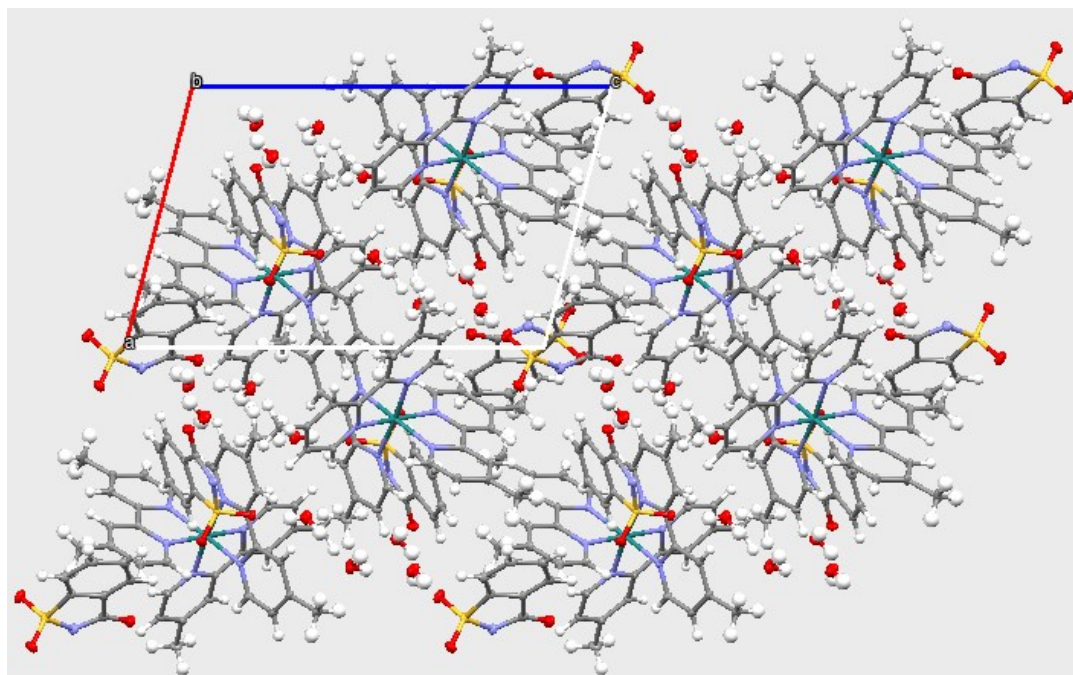


Figure S14 Simulated powder pattern of **2b** with help of the Mercury software¹ based on the single crystal structure of **2b**.

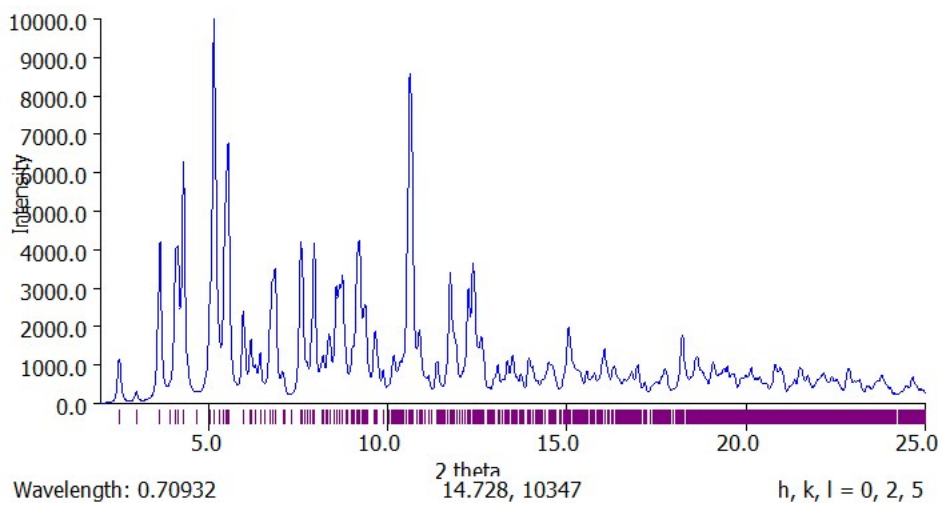
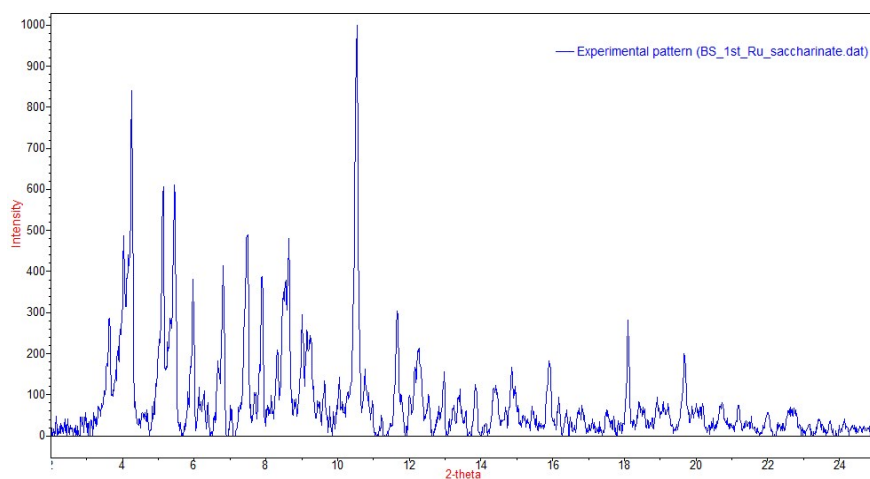


Figure S15 Measured powder XRD pattern of **2b** synthesized on a macroscopic scale as described above.



S6 Cobalt(II) bis(2,2'-bipyrid-6'-yl)ketone *p*-toluenesulfonate tetrahydrate (4a)

Single crystals of **4a** were obtained from the high throughput screening method for nano-crystallization of salts by vapor diffusion at 20°C of 500 nL of a 90% saturated solution of **3** in water mixed with the same volume of a 0.15 M solution of sodium *p*-toluenesulfonate against a reservoir of a 0.15 M solution of sodium *p*-toluenesulfonate. The crystallographic data are summarized in Table S3. During crystallization a ligand exchange took place, in which one bromide ligand was replaced by a *p*-toluenesulfonate ligand and the other bromide ligand by an aqua ligand. **4a** crystallized in the monoclinic space group $P2_1/c$. The coordinated water molecule forms hydrogen bonds to one of the co-crystallized water molecules and to an oxygen atom of the coordinated *p*-toluenesulfonate ligand (O34-H34A O35: 2.640(3) Å, O34-H34A O35B: 2.568(8) Å, O34-H34B O33(x,-1+y,z): 2.7180(19) Å).

Figure S14 Packing diagram of **4a**.

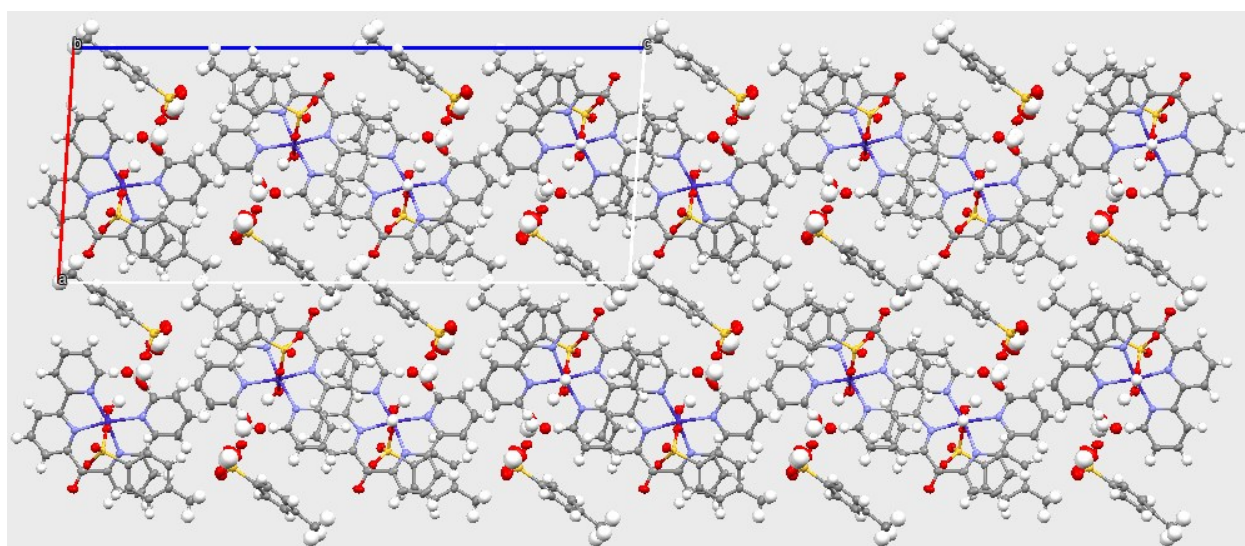


Figure S15 Simulated powder pattern of **4a** with help of the Mercury software¹ based on the single crystal structure of **4a**

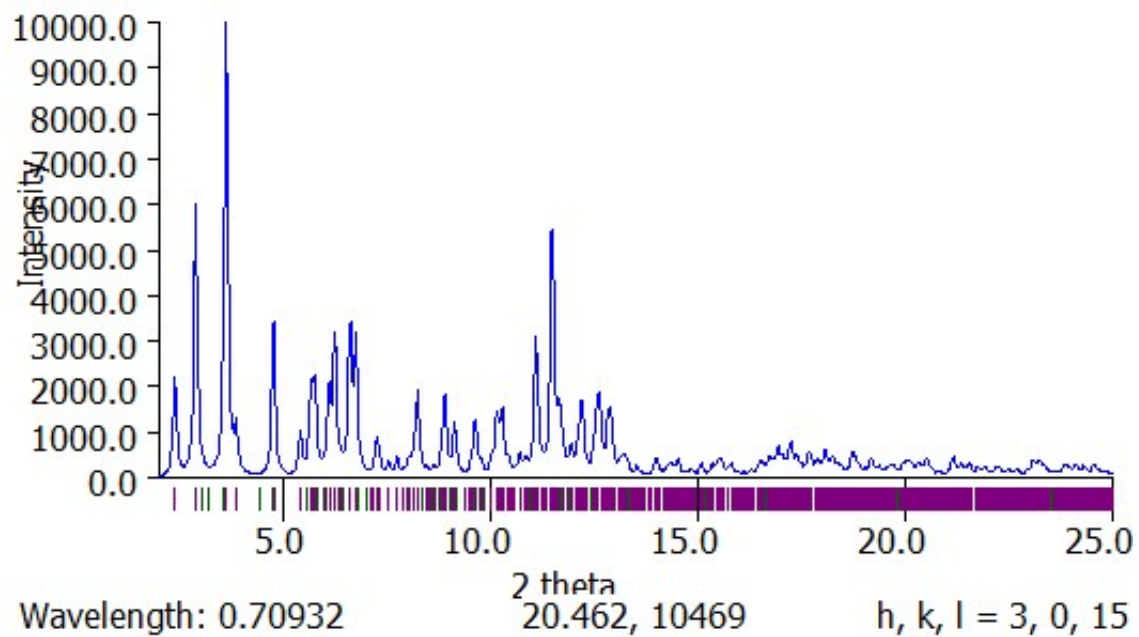
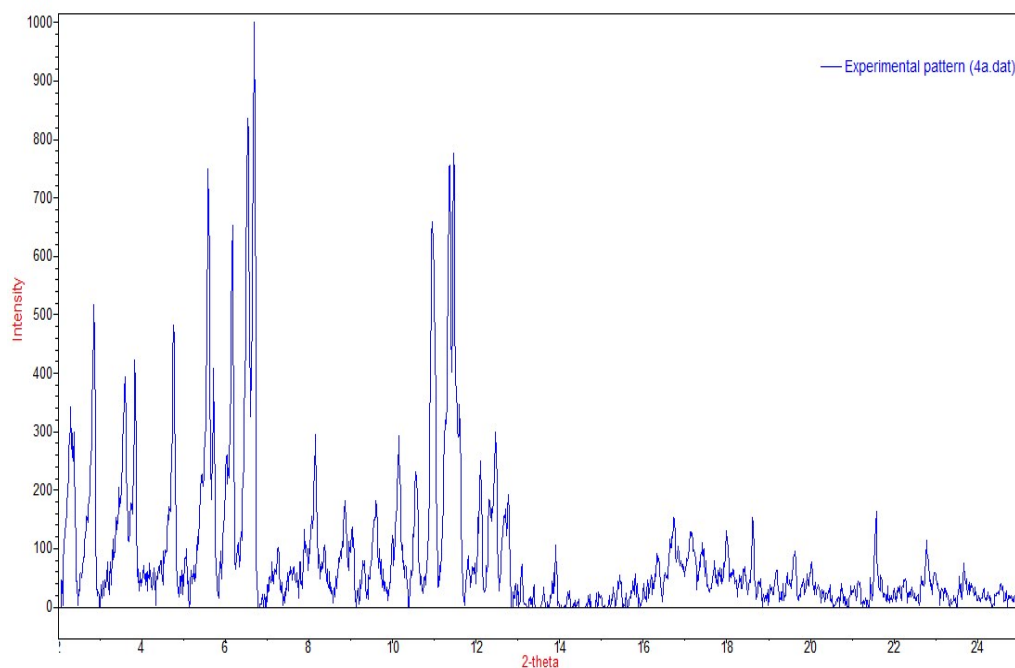


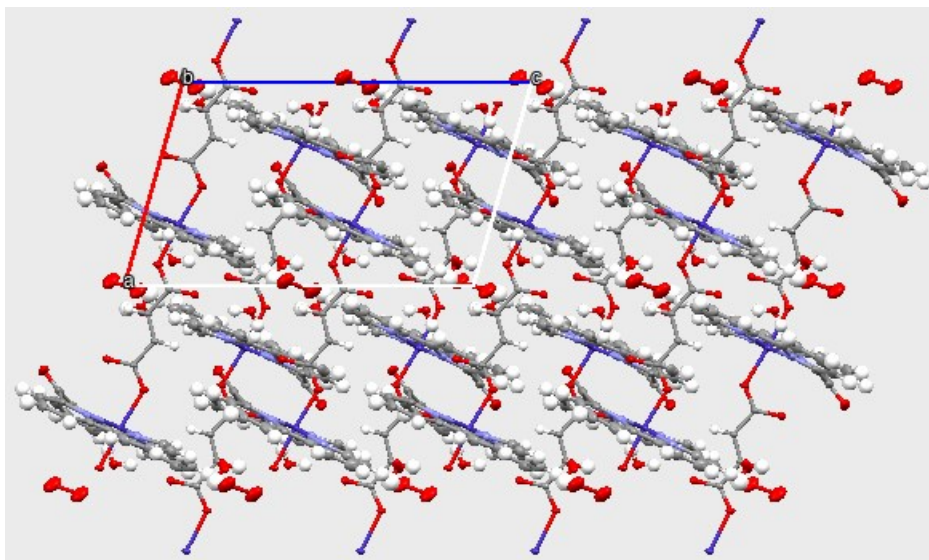
Figure S16 Measured powder XRD pattern of **4a**



S7 Cobalt(II) bis(2,2'-bipyrid-6'-yl)ketone fumarate · 2.25 hydrate (**4b**)

Single crystals of **4b** were obtained from the high throughput screening method for nano-crystallization of salts by vapor diffusion at 20°C of 500 nL of a 90% saturated solution of **3** in water mixed with the same volume of a 0.725 M solution of disodium fumarate against a reservoir of a 0.725 M solution of disodium fumarate. The crystallographic data are summarized in Table S3. During crystallization a ligand exchange took place, whereby the two bromide ligands were replaced by a fumarate anion, which bridges two cobalt metal ions forming 1D-chains. This 1D-coordination polymer runs parallel to the *a*-axis direction. **4b** crystallized in the monoclinic space group $P2_1/c$. The water molecules forms hydrogen bonds to the oxygen atoms of the coordinated fumarate ligand (O35-H35A O33: 2.823(3) Å, O36-H36A O34(x,1.5-y,0.5+z): 2.753(2) Å, O36-H36B O32: 2.779(3) Å).

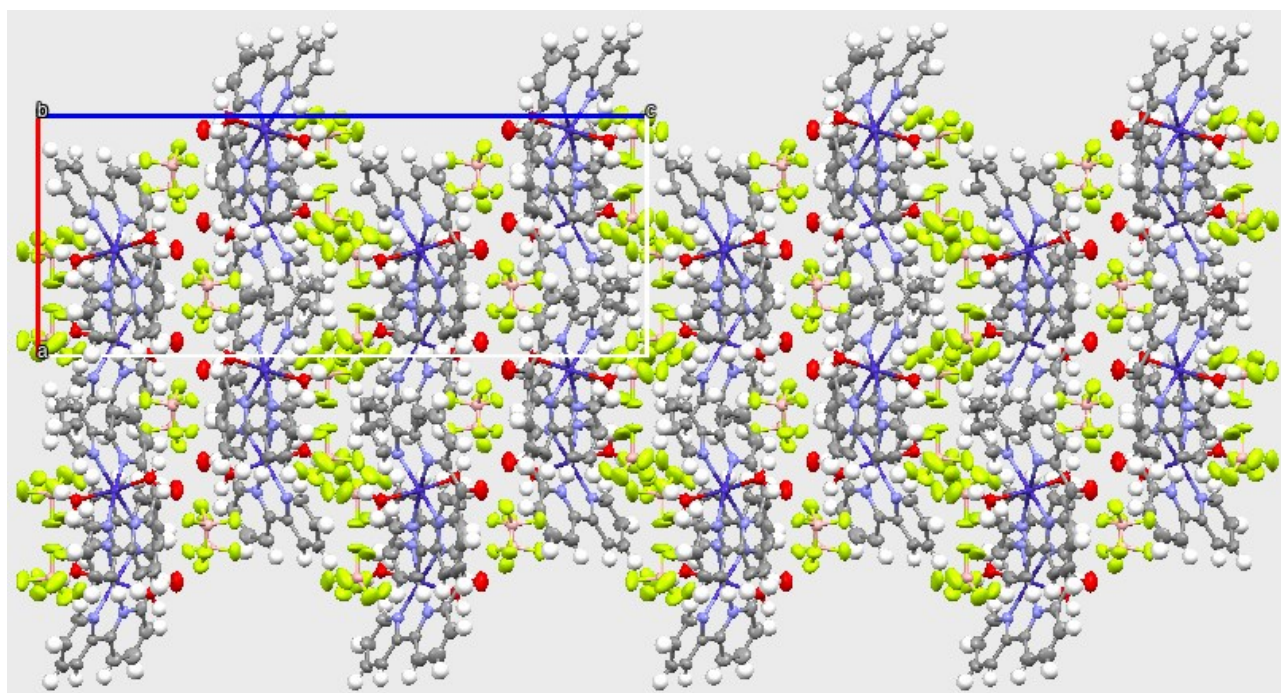
Figure S17 Packing diagram of **4b**.



S8 Cobalt(II) bis(2,2'-bipyrid-6'-yl)ketone tetrafluoroborate dihydrate (4c)

Single crystals of **4c** were obtained from the high throughput screening method for nano-crystallization of salts by vapor diffusion at 20°C of 500 nL of a 90% saturated solution of **3** in water mixed with the same volume of a 2 M solution of sodium tetrafluoroborate against a reservoir of a 2 M solution of sodium tetrafluoroborate. As tetrafluoroborate is known to hydrolyze in water⁶, it is recommended to use a freshly prepared solution. Additionally, the reaction should be done in plastic vessels, as liberated fluoride might react with glassware to yield SiF₆²⁻. The crystallographic data are summarized in Table S3. During crystallization, a ligand exchange took place, whereby both bromide ligands were replaced by aqua ligands. **4c** crystallized in the orthorhombic space group *Pbca*. The asymmetric unit consists of one cobalt(II) bis(2,2'-bipyrid-6'-yl)ketone cation, two coordinated water molecules and two tetrafluoroborate anions. The coordinated aqua ligands form hydrogen bonds to the fluorine atoms of the co-crystallized tetrafluoroborate anion (O2-H2A F1(0.5+x,y,0.5-z): 2.755(2) Å, O2-H2B F2: 2.697(2) Å, O3-H3A F5B(0.5+x, 1.5-y,1-z): 2.737(4) Å, O3-H3B F7B: 2.669(7) Å, O3-H3B F8: 2.647(8) Å).

Figure S18 Packing diagram of **4c**.



S9 Cobalt(II) bis(2,2'-bipyrid-6'-yl)ketone terephthalate tetrahydrate (4d)

Single crystals of **4d** were obtained from the high throughput screening method for nano-crystallization of salts by vapor diffusion at 20°C of 500 nL of a 90% saturated solution of **3** in water mixed with the same volume of a 0.06 M solution of disodium terephthalate against a reservoir of a 0.06 M solution of disodium terephthalate. The crystallographic data are summarized in Table S3. During crystallization a ligand exchange took place, whereby one bromide ligand was replaced by an aqua ligand and the other bromide ligand by a terephthalate dianion, which bridges two cobalt centers across a center of inversion to form a dimer. **4d** crystallized in the triclinic space group $P\bar{1}$. The asymmetric unit consists of one cobalt(II) bis(2,2'-bipyrid-6'-yl)ketone aqua cation with only half of the coordinated terephthalate, four water molecules and another half of a free terephthalate dianion. The coordinated aqua ligand forms hydrogen bonds to a water molecule and to an oxygen atom of the co-crystallized terephthalate anion and other water molecules. Co-crystallized water molecules form hydrogen bonds to the coordinated terephthalate anion and the oxygen atom of the keto group (O2-H2A O41: 2.7642(15) Å, O2-H2B O31: 2.5825(14) Å, O42-H42B O1(x,y,1+z): 2.9496(15) Å, O43-H43A O34: 2.7719(14) Å).

Figure S19 Packing diagram of **4d**.

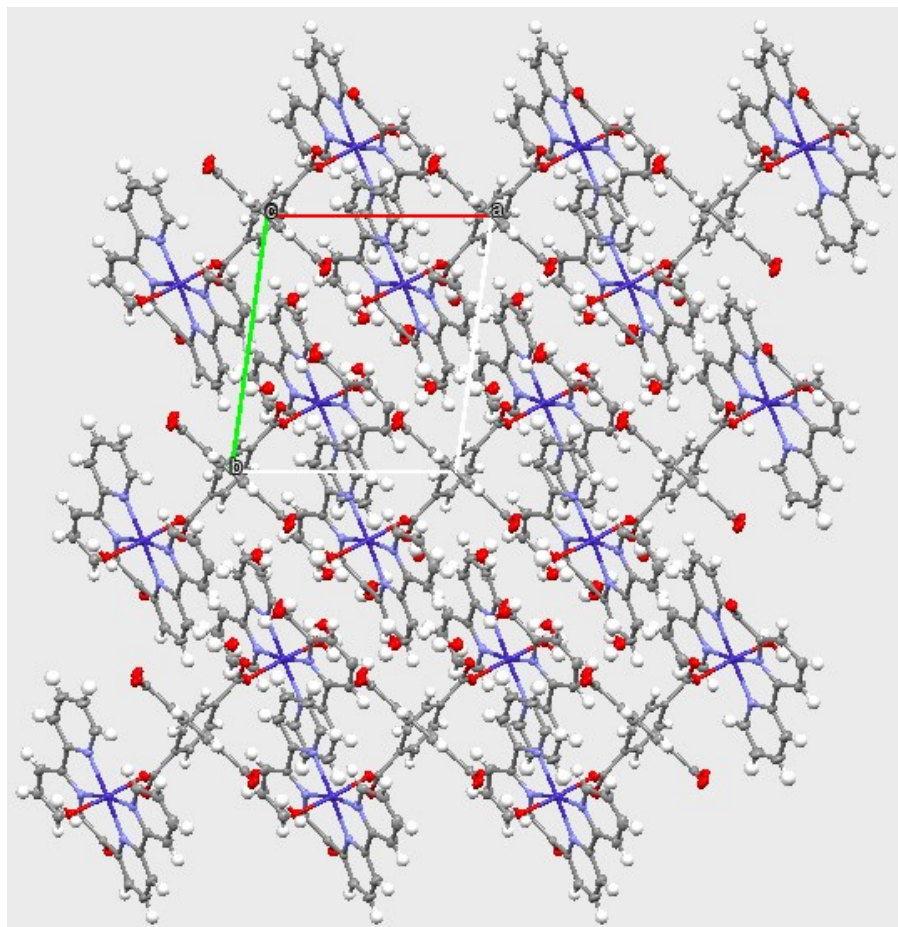


Figure S10 Simulated powder pattern of **4d** with help of the Mercury software¹ based on the single crystal structure of **4d**

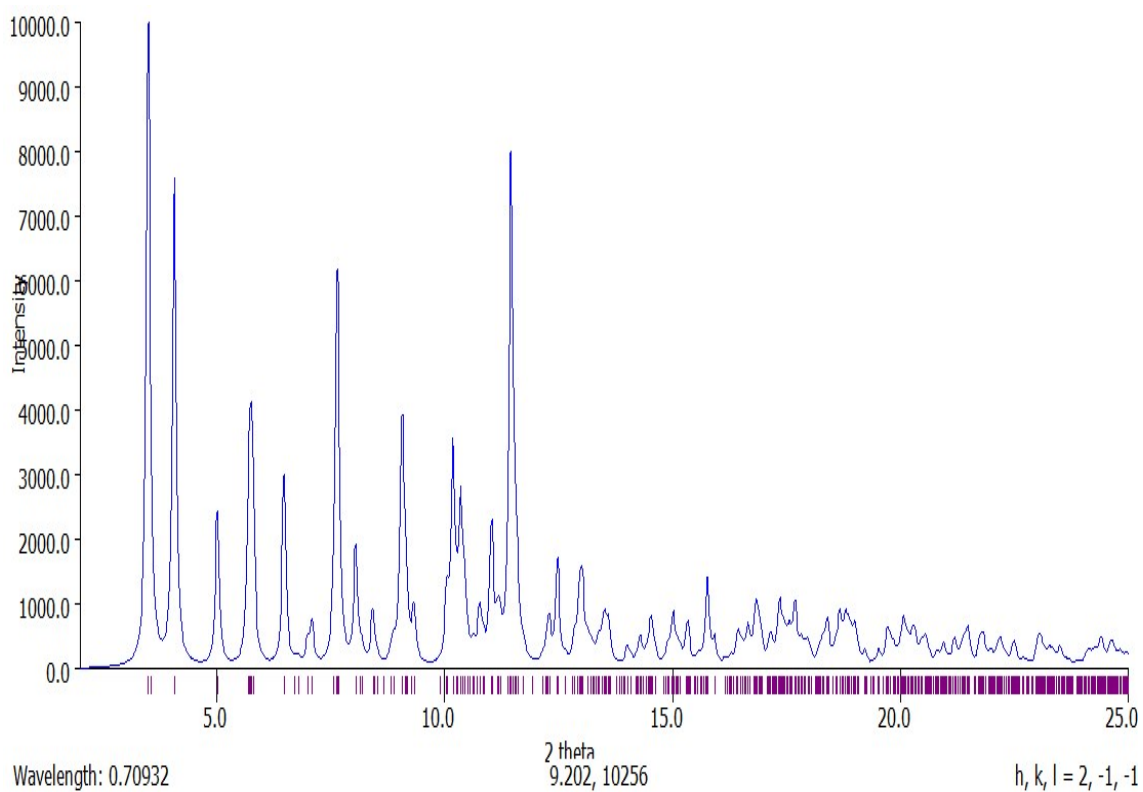


Figure S21 Measured powder XRD pattern of **4d**

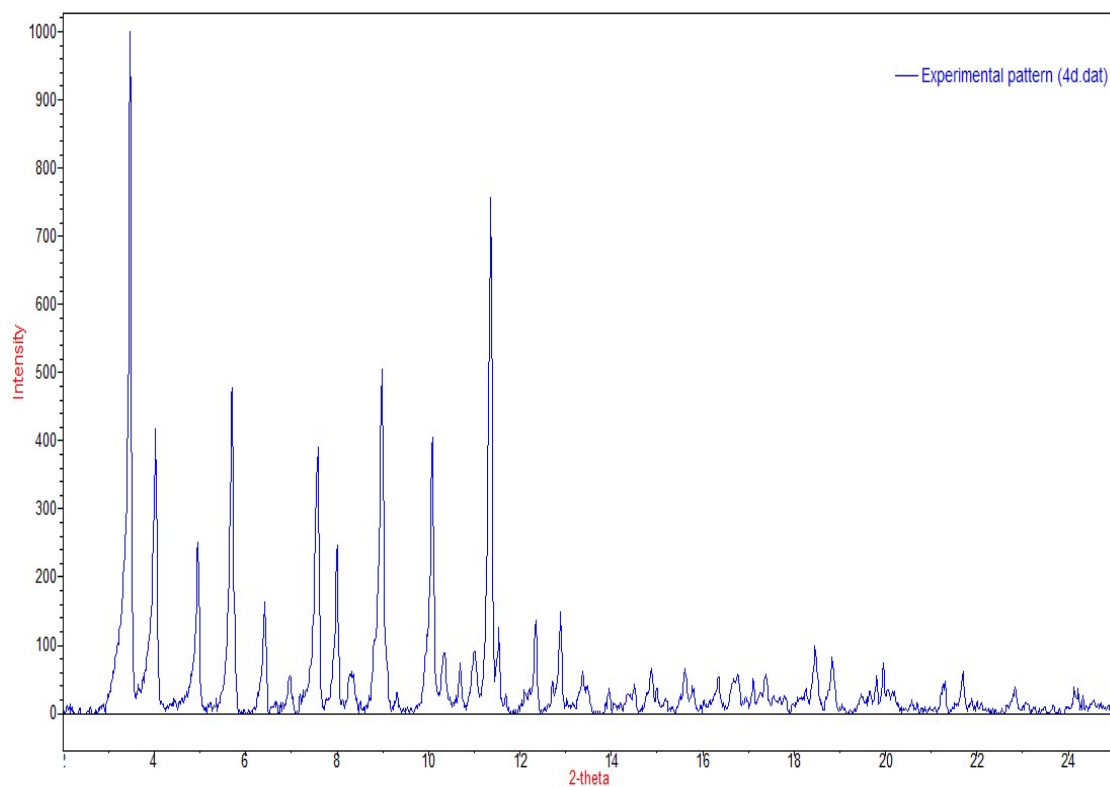


Table S1. Crystal data and structure refinement for **1a**, **1b** and **1c**.

Empirical formula	C ₃₂ H ₃₂ ClCoN ₉ O ₄	C ₂₄ H ₃₉ CoN ₄ O ₁₅	C ₄₈ H ₇₃ Cl _{0.5} Co ₂ N ₈ Na _{0.5} O _{28.5}
Formula weight	701.03	682.52	1365.22
Crystal system	Hexagonal	Monoclinic	Triclinic
Space group	P6/mcc	I2/a	P1
a [Å]	13.2910(3)	11.0119(3)	11.0232(3)
b [Å]	13.2910(3)	19.0675(5)	12.5433(3)
c [Å]	21.3987(5)	14.7124(4)	12.8798(2)
α [°]	90	90	96.573(2)
β [°]	90	99.242(3)	109.779(2)
γ [°]	120	90	109.922(2)
Volume [Å ³]	3273.66(17)	3049.05(14)	1521.44(7)
Z	4	4	1
Dens. (calc.) [Mg/m ³]	1.422	1.487	1.490
Temperature [K]	160.0(1)	160.0(1)	160.0(1)
Wavelength [Å]	1.54184	0.71073	0.71073
Absorption coefficient [mm ⁻¹]	5.292	0.640	0.664
F(000)	1452	1432	713
Crystal size [mm ³]	0.15 x 0.09 x 0.07	0.334 x 0.155 x 0.076	0.214 x 0.139 x 0.096
Crystal description	red block	brownish yellow plate	brownish yellow needle
Theta range for data collection [°]	3.840 to 78.497	2.157 to 33.380	2.147 to 32.031
Index ranges	-16<=h<=14, -16<=k<=16, - 26<=l<=26	-16<=h<=16, -28<=k<=27, - 21<=l<=22	-16<=h<=16, -18<=k<=18, - 19<=l<=19
Refl. collected	1465	35673	87640
Indep. reflections	1465	5416 [R(int) = 0.0454]	20604 [R(int) = 0.0592]
Refl. observed	1358	4592	18139
Comple. to theta	100.0 % to 67.684°	99.9 % to 25.242°	100.0 % to 25.242°
Absorption correction	Semi-empirical from equivalents	Gaussian	Gaussian
Max. and min. transmission	1.00000 and 0.81749	1.000 and 0.532	1.000 and 0.694
Data / restraints /	1465 / 23 / 99	5416 / 6 / 245	20604 / 39 / 885

parameters			
Goodness-of-fit on F^2	1.104	1.049	1.074
Final R indices [$I > 2 \sigma(I)$]	R1 = 0.0456, wR2 = 0.1267	R1 = 0.0651, wR2 = 0.1806	R1 = 0.0630, wR2 = 0.1743
R indices (all data)	R1 = 0.0485, wR2 = 0.1294	R1 = 0.0745, wR2 = 0.1864	R1 = 0.0689, wR2 = 0.1784
Absolute structure parameter	n.a.	n.a.	0.015(8)
Largest diff. peak and hole [$e \cdot \text{\AA}^{-3}$]	0.465 and -0.360	1.354 and -0.708	1.589 and -0.351
CCDC number	1986517	1986518	1986523

Table S2. Crystal data and structure refinement for **2a** and **2b**.

Empirical formula	C ₈₄ H ₉₆ N ₁₂ O ₂₀ Ru ₂	C ₅₀ H ₅₂ N ₈ O ₁₀ RuS ₂
Formula weight	1795.86	1090.18
Crystal system	Monoclinic	Triclinic
Space group	P2 ₁ /n	P-1
a [Å]	10.86902(17)	10.96129(12)
b [Å]	26.9994(3)	14.02802(18)
c [Å]	14.8551(2)	16.6813(2)
α [°]	90	94.3044(10)
β [°]	103.9921(15)	103.1817(10)
γ [°]	90	102.6242(10)
Volume [Å ³]	4229.98(11)	2415.90(5)
Z	2	2
Density (calculated) [Mg/m ³]	1.410	1.499
Temperature [K]	160.0(1)	100.00(11)
Wavelength [Å]	0.71073	0.71073
Absorption coefficient [mm ⁻¹]	0.435	0.480
F(000)	1864	1128
Crystal size [mm ³]	0.278 x 0.117 x 0.063	0.418 x 0.208 x 0.105
Crystal description	red prism	red plate
Theta range for data collection [°]	2.073 to 35.400	2.530 to 35.486
Index ranges	-17<=h<=14, -43<=k<=43, -22<=l<=24	-16<=h<=17, -21<=k<=22, -26<=l<=26
Reflections collected	113527	63275
Independent reflections	17576 [R(int) = 0.0310]	19867 [R(int) = 0.0245]
Reflections observed	14960	17383
Completeness to theta	99.9 % to 25.242°	99.9 % to 25.242°
Absorption correction	Gaussian	Gaussian
Max. and min. transmission	1.000 and 0.503	1.000 and 0.604
Data / restraints / parameters	17576 / 10 / 551	19867 / 0 / 666
Goodness-of-fit on F ²	1.036	1.035
Final R indices [I>2 sigma (I)]	R1 = 0.0407, wR2 = 0.0996	R1 = 0.0307, wR2 = 0.0736
R indices (all data)	R1 = 0.0495, wR2 = 0.1039	R1 = 0.0380, wR2 = 0.0760
Largest diff. peak and hole [e.Å ⁻³]	2.251 and -1.188	0.865 and -0.820
CCDC number	1986525	1986521

Table S3. Crystal data and structure refinement for **4a**, **4b**, **4c** and **4d**.

Empirical formula	C ₃₅ H ₃₄ CoN ₄ O ₁₀ S ₂	C ₂₅ H ₂₀ CoN ₄ O _{7.25}	C ₂₁ H ₁₈ B ₂ CoF ₈ N ₄ O ₃	C ₂₉ H ₂₈ CoN ₄ O ₁₀
Formula weight	793.71	551.38	606.94	651.48
Crystal system	Monoclinic	Monoclinic	Orthorhombic	Triclinic
Space group	P2 ₁ /c	P2 ₁ /c	Pbca	P-1
a [Å]	14.10529(13)	9.89915(12)	11.27579(6)	10.11478(10)
b [Å]	7.34748(6)	14.63676(17)	14.74324(9)	12.22371(13)
c [Å]	34.2057(3)	16.3365(2)	28.71969(18)	12.36967(13)
α [°]	90	90	90	108.5720(9)
β [°]	93.7339(8)	105.9811(13)	90	94.8837(8)
γ [°]	90	90	90	95.9772(8)
Volume [Å ³]	3537.50(6)	2275.53(5)	4774.41(5)	1430.47(3)
Z	4	4	8	2
Density (calc.) [Mg/m ³]	1.490	1.609	1.689	1.513
Temperature [K]	160.00(14)	159.99(10)	160.0(1)	160.0(1)
Wavelength [Å]	1.54184	0.71073	1.54184	1.54184
Absorption coefficient [mm ⁻¹]	5.455	0.813	6.530	5.279
F(000)	1644	1132	2440	674
Crystal size [mm ³]	0.33 x 0.077 x 0.023	0.242 x 0.168 x 0.143	0.187 x 0.121 x 0.009	0.182 x 0.08 x 0.049
Crystal description	light green plate	red prism	brown plate	brown prism
Theta range for data collection [°]	3.140 to 76.651	2.140 to 35.279	3.077 to 78.831	3.800 to 78.834
Index ranges	-17<=h<=17, - 9<=k<=9, - 43<=l<=41	-15<=h<=16, - 23<=k<=23, - 26<=l<=25	-14<=h<=14, - 18<=k<=17, - 36<=l<=36	-12<=h<=12, - 15<=k<=15, - 15<=l<=15
Refl. collected	49213	74322	116931	52740
Indep. reflections	7410 [R(int) = 0.0376]	9547 [R(int) = 0.0255]	5136 [R(int) = 0.0470]	5771 [R(int) = 0.0266]
Refl. observed	6718	8924	4604	5667
Comple. to theta	100.0 % to 67.684°	100.0 % to 25.242°	100.0 % to 67.684°	95.2 % to 67.684°
Absorption correction	Gaussian	Gaussian	Sphere	Semi-empirical from equivalents
Max. and min.	1.000 and 0.421	1.000 and 0.682	0.47800 and 0.42466	1.00000 and 0.71041

transmission				
Data / restraints / parameters	7410 / 1 / 498	9547 / 0 / 359	5136 / 0 / 391	5771 / 0 / 428
Goodness-of-fit on F ²	0.999	1.356	1.076	1.080
Final R indices [I > 2 sigma (I)]	R1 = 0.0316 wR2 = 0.0766	R1 = 0.0607 wR2 = 0.1281	R1 = 0.0396 wR2 = 0.1088	R1 = 0.0233 wR2 = 0.0650
R indices (all data)	R1 = 0.0365 wR2 = 0.0796	R1 = 0.0637 wR2 = 0.1290	R1 = 0.0441 wR2 = 0.1122	R1 = 0.0238 wR2 = 0.0653
Largest diff. peak and hole [e.Å ⁻³]	0.342 and -0.281	0.757 and -0.642	0.568 and -0.374	0.252 and -0.398
CCDC number	1986520	1986519	1986524	1986522

Table S4: Variation of metal-to-metal distances in cobalt(II) bis(2,2'-bipyrid-6'-yl)ketone complexes as a function of the anion, sorted by shortest to longest metal-to-metal distance:

Complex number and axial metal coordination	Cobalt to cobalt distance	Description	Ref.
4d Terephthalate bridged 2 Co, on other side aqua ligand that is bridged by one terephthalate to another aqua ligand	6.8324(3) 8.3070(3) 8.7763(4) 9.2150(3) 10.1148(3) 11.1848(4)	neighbouring columns neighbouring columns neighbouring columns neighbouring columns neighbouring columns bridged by one terephthalate	This work
4a Tosylate on one side, aqua ligand on the other	7.3475(3) 7.8620(9) 8.5396(8) 11.1939(9)	Aqua ligand bonded to tosylate coordinated to Co neighbouring columns neighbouring columns neighbouring columns	This work
4c Aqua ligand bound on each side	7.9998(8) 8.5397(4) 9.0415(7) 10.1413(4) 10.1959(7) 10.2998(6) 11.2758(5)	neighbouring columns neighbouring columns BF ₄ bridges two aqua ligands neighbouring columns BF ₄ bridges linearly two aqua ligands neighbouring columns neighbouring columns	This work
cobalt(II) bis(2,2'-bipyrid-6'-yl)ketone (ClO ₄) ₂ Aqua ligands on each side	8.0982(9) 8.679(1) 9.170(1) 10.294(1) 11.354(1)		7
4b Fumarate anions on each axial side	8.1800(5) 8.1823(4) 9.8168(4) 9.8991(5) 10.3301(5) 10.9326(5) 10.9718(4)	neighbour. columns (U turn of fumarate – H ₂ O - carboxylate) neighbouring columns neighbouring columns bridged by one fumarate neighbouring columns neighbouring column (bridged by carboxylate - H ₂ O carboxylate)	This work
cobalt(II) bis(2,2'-bipyrid-6'-yl)ketone (OTf) ₂ 2 molecules in asym unit. OTf on each side	8.2128(7) 8.2877(7) 8.5950(6) 8.6187(3) 8.9420(7) 9.9498(6) 9.8828(7) 10.6636(6)	distance between the two metal centres in the a.u.	8

	10.7931(7)		
	11.4584(6)		
	11.8633(7)		

References

1. C. F. Macrae, L. Sovago, S. J. Cottrell, P. T. A. Galek, P. McCabe, E. Pidcock, M. Platings, G. P. Shields, J. S. Stevens, M. Towler and P. A. Wood, *J. Appl. Cryst.*, 2020, **53**, 226-235.
2. L. Prieto, M. Neuburger, B. Spingler and F. Zelder, *Org. Lett.*, 2016, **18**, 5292-5295.
3. a) P. Kraft, A. Bergamaschi, C. Broennimann, R. Dinapoli, E. F. Eikenberry, B. Henrich, I. Johnson, A. Mozzanica, C. M. Schlepütz, P. R. Willmott and B. Schmitt, *J. Synchrotron Rad.*, 2009, **16**, 368-375; b) C. Brönnimann and P. Trüb, in *Synchrotron Light Sources and Free-Electron Lasers: Accelerator Physics, Instrumentation and Science Applications*, eds. E. J. Jaeschke, S. Khan, J. R. Schneider and J. B. Hastings, Springer International Publishing, Cham, 2016, pp. 995-1027; c) A. Förster, S. Brandstetter and C. Schulze-Briese, *Philos. Trans. R. Soc. A*, 2019, **377**, 20180241.
4. W. Liu, W. Xu, J.-L. Lin and H.-Z. Xie, *Acta Cryst.*, 2008, **E64**, m1586-m1586.
5. A. L. Spek, *Acta Cryst.*, 2015, **C71**, 9-18.
6. M. G. Freire, C. M. S. S. Neves, I. M. Marrucho, J. A. P. Coutinho and A. M. Fernandes, *J. Phys. Chem. A*, 2010, **114**, 3744-3749.
7. J. C. Knight, A. J. Amoroso, P. G. Edwards, R. Prabakaran and N. Singh, *Dalton Trans.*, 2010, **39**, 8925-8936.
8. S. Schnidrig, C. Bachmann, P. Müller, N. Weder, B. Spingler, E. Joliat-Wick, M. Mosberger, J. Windisch, R. Alberto and B. Probst, *ChemSusChem*, 2017, **10**, 4570-4580.